Marine Pollution Bulletin 95 (2015) 305–314

Contents lists available at ScienceDirect

Marine Pollution Bulletin

journal homepage: www.elsevier.com/locate/marpolbul

# Microplankton dynamics under heavy anthropogenic pressure. The case of the Bahía Blanca Estuary, southwestern Atlantic Ocean

M. Celeste López Abbate [a,*], Juan Carlos Molinero [b], Valeria A. Guinder [a], M. Sofía Dutto [a], M. Sonia Barría de Cao [a], Laura A. Ruiz Etcheverry [c], Rosa E. Pettigrosso [d], M. Cecilia Carcedo [a], Mónica S. Hoffmeyer [a,e]

[a] Instituto Argentino de Oceanografía, IADO CONICET, Camino La Carrindanga km 7.5, 8000 Bahía Blanca, Argentina
[b] GEOMAR Helmholtz Centre for Ocean Research Kiel, Marine Ecology/Food Webs, Düsternbrooker Weg 20, 24105 Kiel, Germany
[c] Departamento de Ciencias de la Atmósfera y los Océanos, FCEN UBA, Ciudad Universitaria, 1428 Buenos Aires, Argentina
[d] Universidad Nacional del Sur, Laboratorio de Ecología Acuática, San Juan 670, 8000 Bahía Blanca, Argentina
[e] Universidad Tecnológica Nacional, Facultad Regional Bahía Blanca, 11 de Abril 461, 8000 Bahía Blanca, Argentina

ARTICLE INFO

*Article history:*
Available online 30 March 2015

*Keywords:*
Microplankton
Eutrophication
Estuaries
Nutrient stoichiometry
Climate
Path analysis

ABSTRACT

Quantifying biotic feedbacks in response to environmental signals is fundamental to assess ecosystem perturbation. We analyzed the joint effects of eutrophication, derived from sewage pollution, and climate at the base of the pelagic food web in the Bahía Blanca Estuary (SW Atlantic Ocean). A two-year survey of environmental conditions and microplankton communities was conducted in two sites affected by contrasting anthropogenic eutrophication conditions. Under severe eutrophication, we found higher phytoplankton abundance consistently dominated by smaller sized, non siliceous species, while microzooplankton abundance remained lower and nutrient stoichiometry showed conspicuous deviations from the Redfield ratio. Phytoplankton growth in such conditions appeared controlled by phosphorous. In turn, microplankton biomass and phytoplankton size ratio (<20 μm:>20 μm) displayed a saturation relationship with nutrients in the highly eutrophic area, although mean phytoplankton growth was similar in both eutrophic systems. The strength of links within the estuarine network, quantified through path analysis, showed enhanced relationships under larger anthropogenic eutrophication, which fostered the climate influence on microplankton communities. Our results show conspicuous effects of severe sewage pollution on the ecological stoichiometry, i.e., N and P excess with respect to Si, altering nutrient ratios for microplankton communities. This warns on wide consequences on food web dynamics and ultimately in ecosystem assets of coastal pelagic environments.



## 1. Introduction

Estuaries are exposed to multiscale biotic and abiotic factors heavily affected by anthropogenic forces. Among human induced environmental changes, coastal eutrophication constitutes a major challenge to these ecosystems due to the consequences on biomass and structure at the base of food webs. In addition, eutrophication is likely to increase in the near future along with enhanced anthropogenic activities in coastal areas (Rabalais, 2004). The cumulative effect of climate change (i.e. ocean warming and acidification, sea level rise) and the occurrence of sudden climate events (i.e. extreme rainfall, drought, flooding) therefore warn on the potential vulnerability of estuarine systems (Paerl et al., 2006; Rabalais et al., 2009). Long term environmental surveys that integrate the entire trophic network are therefore essential to supply reliable data to quantitatively assess, and eventually forecast, the impact of anthropogenic and climate disturbances in estuaries.

Nutrient loading in coastal habitats promotes an increase in the magnitude and frequency of phytoplankton blooms (Cloern, 2001). Irregular nutrient pulses result in the occurrence of discrete productivity events, which may be accompanied by a trophic mismatch (Strom, 2002). An increase in phytoplankton biomass due to nutrient loading is associated with changes in the elemental stoichiometry of cells. Depending on the environmental ratio of nutrients, the C:nutrients ratio of phytoplankton community may shift affecting food quality for primary consumers (Sterner and Elser, 2002; Elser et al., 2010). Eventually these changes propagate throughout the entire food web, as the grazing potential of

* Corresponding author. Tel./fax: +54 0291 4861112.
*E-mail address:* mclabbate@iado-conicet.gob.ar (M.C. López Abbate).

http://dx.doi.org/10.1016/j.marpolbul.2015.03.026
0025-326X/

consumers determines the magnitude of phytoplankton biomass accumulation and the energy transfer in the pelagic environment.

The Bahía Blanca Estuary is a highly productive and eutrophic ecosystem in the southern Atlantic Ocean, heavily impacted by anthropogenic activities (Marcovecchio et al., 2008). Industrial and domestic waste is being dumped in the inner estuary, while human activities are rapidly growing in the area. Consequently, coastal eutrophication in the inner estuary appears responsible of a considerable reduction on zooplankton abundance and diversity (Barría de Cao et al., 2003; Biancalana et al., 2012; Dutto et al., 2012). Eutrophication effects on zooplankton may further magnify the climate influence, which affects both the physical environment of plankton, as well as the physiological rates of these organisms. Indeed, changes in phenology and structure of phytoplankton and zooplankton, i.e. timing of seasonal peak, species composition and cell sizes, have been ascribed to regional climate modifications (Hoffmeyer, 2004; Guinder et al., 2010, 2013).

Joint effects of multiscale environmental signals shape the structural and functional outcome of populations, and have the potential to move the entire ecosystem towards alternative stable states (Scheffer and Carpenter, 2003). In particular, plankton is sensitive to a wide range of biophysical variables, and can quickly transfer environmental signals into the pelagic food web (Prairie et al., 2012). Their effect however may be either buffered, through compensatory dynamics (Gonzalez and Loreau, 2009), or amplified via trophic tunneling (Taylor et al., 2002). Hence, to resolve how eutrophication gradients modify the pelagic configuration at the base of the food web requires the quantification of interlinks and biotic feedbacks in the estuarine network. We here investigate the microplankton dynamics under varying anthropogenic pressures in the Bahia Blanca Estuary, and test the hypothesis that heavy eutrophication magnify climate effects on microplankton communities, further modifying the network links at the base of pelagic food webs.

## 2. Materials and methods

### 2.1. Study area

The Bahía Blanca Estuary (38°45′–39°40′S, 61°45′–62°30′W) is located in the south western Atlantic Ocean coast, Argentina (Fig. 1). This area shows a temperate climate, marked seasonality and relatively low annual rainfall (ca. 613 mm) that mainly occurs during spring and autumn (Montecinos et al., 2000). The estuary shows inverted salinity gradient as it experience low influence from continental drainage (annual mean 2.7 $m^3 s^{-1}$), high evaporation rate and restricted water circulation in the inner reach (Perillo et al., 2001). Salinity in the inner and middle estuary range between 17.9 and 41.3, and appear driven by the variability of

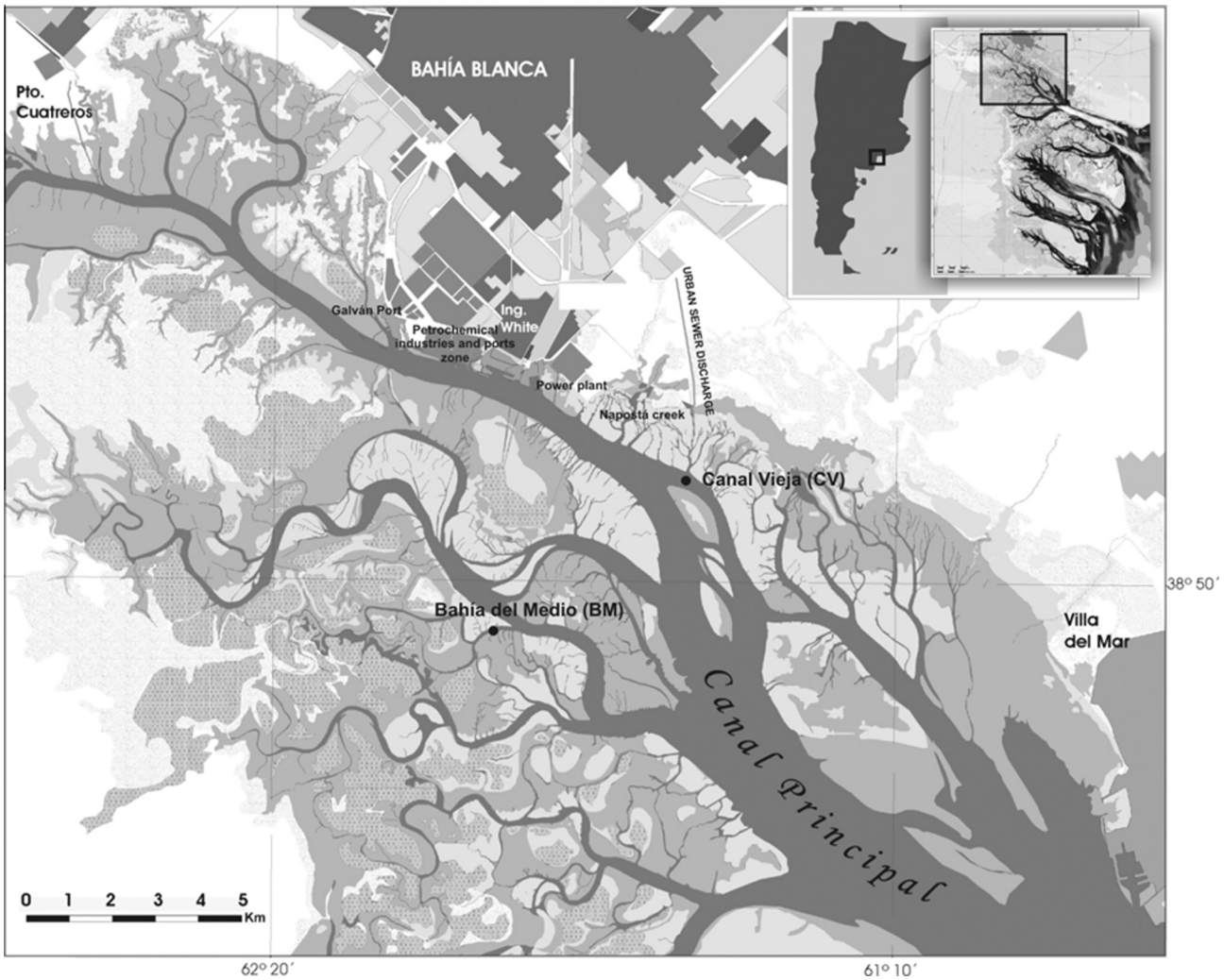


**Fig. 1.** Sampling area showing the location of the highly impacted site "Canal Vieja" (CV) and the control site "Bahía del Medio" (BM).

rainfall, wind and temperature (Freije et al., 2008). The estuary shows a mesotidal regime (mean tidal amplitude 3.5 m) and the water column is highly turbid and non-stratified (Perillo et al., 2001). The estuarine system harbor large tidal flats and salt marshes bordered by shallow channels. High loads of organic matter and nutrients are provided by land and *in situ* biological productivity (Freije et al., 2008).

The sampling stations are located in the inner reach of the estuary (Fig. 1). We used two sites of contrasting conditions in regards to their exposure to anthropogenic stressors (i.e. sewage inputs): a control site, Bahía del Medio (BM), harbored from direct human stress, and a second site, Canal Vieja (CV), directly affected by sewage pollution. The former is located in a narrow, tidal channel non-exposed to human activities (Baldini et al., 1999; Hoffmeyer and Barría de Cao, 2007). The high tidal amplitude along with the morphological features of the channel (mean depth and width of 4.5 and 70 m respectively) promotes the occurrence of high concentrations of suspended matter in the water column (Borel and Gómez, 2006). In contrast, CV, is located adjacent to the Bahía Blanca city (300,000 inhab.) sewage outfall. This effluent represents the 23.3% of total freshwater input to the estuary and significantly contributes with nutrients and organic matter loads (Lara et al., 1985; Barría de Cao et al., 2003; Biancalana et al., 2012; Dutto et al., 2012). The channel receiving this effluent is 300-m wide and has a mean depth of 6.5 m.

### 2.2. Data collection and samples processing

Precipitation data (i.e. monthly rainfall level) were obtained from a station adjacent to the estuary in the Bahía Blanca City, and provided by the Center for Renewable Natural Resources of the Semiarid Zone, CERZOS-CONICET. Field sampling was carried out onboard of a motor boat in daytime during fourteen surveys, from July 2008 to November 2010. *In situ* temperature, pH, dissolved oxygen and salinity were measured by means of a multiparametric probe Horiba U-10. Samples for chemical and microplanktonic analyses were taken from the surface layer during the middle ebb tide. Water samples (500 ml) were filtered through 0.7 μm GF/F filters for the estimation of chlorophyll *a*. Size fractionated chlorophyll *a* (<135 and <20 μm) was determined by a spectrophotometer as described in Lorenzen and Jeffrey (1980). These measures were used to assess the ratio phytoplankton biomass ($\mu g\, C\, l^{-1}$) – chlorophyll *a* from each size fraction (C:Chl*a*). To avoid large grazers and given that most of the phytoplankton in the inner estuary is below the 100 μm size fraction (e.g. Guinder et al., 2010), we used a smaller than usual pore size (135 μm) for size fractionation. A number of 2–4 replicates of seawater samples were analyzed to estimate the concentration of dissolved nitrate, nitrite, ammonium, phosphate, and silicate using a Technicon AA-II Autoanalyzer expanded to five channels, as described in APHA-AWWA-WEF (1998).

To quantify nanoflagellates, phytoplankton and microzooplankton, a variable volume (10–50 ml, depending on sediment and plankton concentration) of preserved seawater sample (Lugol's iodine) was settled in Utermöhl chambers during 24 h. The entire chamber was analyzed under a Wild M20 inverted microscope (Hasle, 1978). Identification of micro-sized plankton was to the lowest possible taxon. For this porpoise, samples were collected using a Nansen 30 μm net and preserved with formaldehyde (final concentration 0.4%). Afterwards, plankton was analyzed using a Zeiss Standard R microscope and a Nikon Eclipse microscope, with magnification of 1000× and phase contrast. Nano-sized organisms were counted using the same methodology applied to quantified micro-sized phytoplankton, i.e., settled in Utermöhl chambers and analyzed under inverted microscope. This technique however, does not allow the correct identification of species and therefore, the discrimination amongst autotrophs and heterotrophs was not feasible. Regarding this methodological constrain, we include all nano-sized flagellates into one category (nanoflagellates). Phytoplankton and microzooplankton cell volumes were calculated assigning simple geometric shapes to species (Hillebrand et al., 1999), and converted into carbon content ($\mu g\, C\, l^{-1}$) according to Menden-Deuer and Lessard (2000).

The rates of phytoplankton growth ($\mu$) and mortality ($m$) due to microzooplankton grazing was calculated based on the dilution method as described by Landry and Hassett (1982). Five replicates of seawater dilution treatments (0%, 25%, 50% and 75%) were incubated *in situ* during 24 h without nutrient addition. Changes of phytoplankton abundance during the incubation were estimated by chlorophyll *a* measurements.

### 2.3. Data analysis

The pelagic environment in estuarine systems is affected by precipitation events, which promote disturbance effects in the water column (e.g. changes in the nutrient cycle and in the water column structure). To detect significant changes in water conditions, we assessed the environmental variability associated to precipitations. The rationale to do so is based on the disturbance effect precipitation events may favor. To detect significant changes in precipitation level during the sampling period (2008–2010) we used the generalized Mahalanobis distance ($D^2$). This is a dimensionless statistic that allows identifying anomalous events in time series (Ibanez, 1981). The general pattern of nutrients was obtained by principal components analysis (PCA) of the standardized (zero mean, unit standard deviation) nutrients matrix. The nutrient matrix included nitrite, nitrate, phosphate and silicate. All these variables appear closely coupled with the annual pattern of rainfall (Spetter et al., 2015; this study). In contrast, the ammonium concentration follows the pattern of sewage flow, as deduced by the high correlation with lithogenic compounds (Lara et al., 1985), and we therefore discarded ammonium from this analysis. The pattern was represented by the first two components which accounted for most of the variability; PC1 (64% and 85% of extracted variance in CV and BM, respectively) and PC2 (29% and 10% of extracted variance in CV and BM, respectively). The first PC was used as a proxy of the trophic state of the system. The relative concentration of nutrients was calculated in order to compare the nutrient ratio in both sites with the Redfield ratio of nutrients (Redfield et al., 1963). The concentration of dissolved inorganic nitrogen (DIN) was calculated as the sum of nitrite, nitrate and ammonium.

Differences of biotic and abiotic variables between sites were calculated by the non-parametric Mann–Whitney U-test. This test was also used to compare the concentration of inorganic nutrients during the period after heavy rainfall (March–May 2010) and the mean value for the whole period (July 2008–November 2010). Differences in the structure, i.e. taxonomic composition of phytoplankton and microzooplankton, between sites were assessed by non-metric Multi-Dimensional Scaling (MDS). The technique was based on triangular matrix using the Bray Curtis similarity index (Clarke and Warwick, 1994). Significant differences in the plankton structure between sites were calculated by a one-way analysis of similarities (ANOSIM) at a significance level of $p < 0.05$ and R statistic >0.5. Similarity percentages analysis (SIMPER) was used to assess the contribution of each species to the similarity within groups and dissimilarity between groups (Clarke and Gorley, 2006). These analyses were performed with PRIMER 6.

The influence of environmental variables and nutrients content on plankton variability was assessed by means of regression analysis. First, the general trend of plankton biomass was depicted by

principal components analysis on the standardized data matrix including nanophytoplankton (cell size <20 μm), microphytoplankton (cell size >20 μm) and microzooplankton biomass (μg C $l^{-1}$). Also, the relative abundance of the size fractions of phytoplankton was estimated as the ratio nano:micro-phytoplankton (hereafter phytoplankton size-fraction ratio). The phytoplankton size fraction ratio and the general trend of plankton biomass were then confronted to environmental variables and nutrient concentration.

To gain further understanding of the Bahia Blanca estuarine system we used path analysis to investigate the strength of links in the estuarine network. The a priori structure of the path model is based on the hypothesis that climate and nutrient loading jointly drive the physical microplankton environment, thereby shaping the structure and functioning of these communities; the strength of links however might vary in concomitance with the exposure to eutrophication magnitude. For each location (i.e. eutrophication condition) specific effects of hydrography and nutrient loading and their co-variations on microplankton biomass were assessed using variance partitioning and explored through path analysis (Peres-Neto et al., 2006). The strength of the links and the quantification of the overall model were determined by simple and partial multivariate regression and Monte Carlo permutation tests (1000 replicates), while the Bayesian Information Criterion (BIC) and Chi-square values were used to assess the robustness of models (Alsterberg et al., 2013). Path coefficients indicate the strength of the relation between causal and response variables. Path analysis was performed using the R library sem.

## 3. Results

### 3.1. Environmental conditions at the sampling sites

Temporal variability of environmental conditions, phytoplankton growth rate and plankton biomass are shown in Table 1. Temperature, pH and turbidity were similar in both sites, however, salinity values and the concentration of dissolved oxygen, pigments, nutrients and particulate organic carbon were significantly different between sites (Mann–Whitney U-test, $p < 0.05$). During the period investigated, a heavy rain period was detected from November 2009 to March 2010 (Fig. 2a). The accumulated precipitation during spring 2009 was 133.6 mm, while in summer 2010, was 205.2 mm. The highest monthly value was reached in February 2010 (90.4 mm). The concentration of dissolved nutrients showed remarkably high concentrations from February to May 2010, following the occurrence of positive precipitation anomalies noticed from November 2009 to March 2010 (Fig. 2b). The concentration of all nutrients after the rainfall pulse (except for ammonium), was significantly higher compared with the mean value of the whole period (Mann–Whitney $U$ Test, BM: nitrite: $U = 9.5$, $p = 0.026$; nitrate: $U = 4.5$, $p = 0.011$; phosphate: $U = 7.5$, $p = 0.019$; silicate: $U = 8.5$, $p = 0.022$; CV: ammonium: $U = 9.0$, $p = 0.029$, nitrite: $U = 8.0$, $p = 0.022$; nitrate: $U = 1.0$, $p = 0.006$; phosphate: $U = 19.0$, $p = 0.113$; silicate: $U = 2.0$, $p = 0.007$). Ammonium concentration showed no clear response after the heavy rainfall event. In BM, the concentration of phosphate and silicate was mainly above the Redfield ratio when compared with DIN. In turn, in CV the concentration of both nutrients was frequently below the Redfield ratio (Fig. 3).

### 3.2. Plankton community

Chlorophyll *a* and phaeopigments concentration was significantly higher in BM (Mann–Whitney U-test, $p < 0.05$). Phytoplankton was characterized by small sized diatoms and cell abundance was significantly higher in CV (Mann–Whitney $U$-test, $p < 0.05$). This difference was mainly due to the higher concentration of nanophytoplankton (<20 μm) in CV (mean = 391.35 × $10^3$ cell $l^{-1}$) in comparison with the concentration in BM (mean = 255.66 × $10^3$ cell $l^{-1}$, Mann–Whitney $U$-test, $p < 0.05$). The concentration of microphytoplankton (>20 μm) was similar in both sites. Nanophytoplankton was the dominant size fraction

**Table 1**
Values of temperature ($T$, °C), salinity (Sal), dissolved oxygen (DO, mg $l^{-1}$), turbidity (Turb, NTU), nutrients (μM), chlorophyll *a* (chl *a*, μg $l^{-1}$), phytoplankton growth rate ($\mu$, $d^{-1}$) and microphytoplankton (MP), nanophytoplankton (NP) and microzooplankton (MZ) biomass ($\mu$ g C $l^{-1}$) during the sampling dates in both sites.

| Site | Date | T | Sal | DO | Turb | Amonio | Nitrite | Nitrate | Phosphate | Silicate | Chl *a* | $\mu$ | MP | NP | MZ |
|---|---|---|---|---|---|---|---|---|---|---|---|---|---|---|---|
| BM | July-08 | 9.00 | 38.30 | 6.77 | 41.00 | 2.03 | 0.28 | 0.16 | 1.31 | 52.37 | 3.90 | 1.97 | 3.13 | 0.61 | 22.15 |
| | December-08 | 23.35 | 38.80 | 7.19 | 43.50 | 8.55 | 0.05 | 0.93 | 1.73 | 70.34 | 10.75 | 0.48 | 44.89 | 10.32 | 29.02 |
| | February-09 | 23.61 | 40.00 | 5.82 | 87.80 | 17.21 | 0.40 | 1.47 | 1.88 | 62.48 | 8.67 | 1.22 | 45.91 | 26.53 | 32.63 |
| | July-09 | 6.85 | 39.00 | 7.33 | 124.00 | 24.57 | 0.07 | 0.15 | 1.16 | 33.25 | 8.49 | 0.00 | 70.59 | 4.48 | 6.85 |
| | August-09 | 11.91 | 39.00 | 5.89 | 46.95 | 35.90 | 0.04 | 0.31 | 1.20 | 40.81 | 3.02 | 0.02 | 55.79 | 7.25 | 100.82 |
| | October-09 | 15.94 | 30.00 | 6.53 | 94.50 | 1.90 | 0.06 | 0.01 | 0.97 | 51.19 | 14.61 | 0.51 | 8.26 | 2.32 | 7.75 |
| | November-09 | 15.86 | 36.60 | 6.53 | 63.50 | 1.83 | 0.11 | 0.01 | 1.31 | 55.01 | 7.11 | 0.28 | 34.49 | 5.49 | 10.05 |
| | March-10 | 15.86 | 36.60 | 6.53 | 63.50 | 34.21 | 2.62 | 5.33 | 2.78 | 102.23 | 8.13 | 1.55 | 29.95 | 3.95 | 10.76 |
| | March-10 | 18.63 | 34.00 | 5.36 | 131.75 | 6.14 | 2.79 | 8.86 | 3.12 | 67.27 | 3.57 | 1.61 | 14.29 | 4.94 | 20.64 |
| | May-10 | 12.10 | 40.00 | 5.41 | 117.50 | 5.92 | 1.66 | 14.76 | 3.77 | 126.11 | 5.58 | 1.20 | 15.91 | 5.09 | 18.43 |
| | July-10 | 6.51 | 37.30 | 7.29 | 202.00 | 3.48 | 0.27 | 1.86 | 2.07 | 53.85 | 8.03 | 0.19 | 10.67 | 0.55 | 12.60 |
| | August-10 | 6.93 | 37.60 | 8.71 | 211.00 | 6.95 | 0.14 | 0.01 | 1.46 | 39.84 | 5.28 | 0.50 | 48.09 | 11.72 | 4.10 |
| | October-10 | 16.05 | 38.50 | 6.02 | 160.00 | 2.01 | 0.87 | 3.40 | 2.62 | 62.16 | 8.64 | – | 26.55 | 7.21 | 28.98 |
| | November-10 | 17.12 | 36.85 | 6.11 | 208.50 | 7.00 | 1.92 | 4.73 | 2.40 | 57.57 | 2.26 | 0.30 | 13.46 | 5.04 | 14.02 |
| CV | July-08 | 12.40 | 34.20 | 7.50 | 109.00 | 64.98 | 0.18 | 0.47 | 5.50 | 52.61 | 3.70 | 2.36 | 30.81 | 2.31 | 4.63 |
| | December-08 | 20.90 | 39.00 | 5.36 | 79.00 | 22.61 | 3.20 | 8.91 | 2.71 | 88.98 | 7.47 | 0.29 | 17.11 | 39.47 | 15.34 |
| | February-09 | 24.25 | 39.50 | 8.05 | 36.50 | 35.13 | 2.49 | 6.05 | 1.97 | 59.79 | 6.20 | 0.00 | 18.52 | 42.15 | 26.22 |
| | July-09 | 7.47 | 39.40 | 6.35 | 63.00 | 68.80 | 0.24 | 2.03 | 2.67 | 34.53 | 13.46 | 0.00 | 87.53 | 5.60 | 4.50 |
| | August-09 | 13.94 | 38.50 | 5.69 | 38.13 | 151.50 | 0.25 | 1.01 | 4.29 | 50.98 | 6.05 | 0.00 | 27.53 | 3.40 | 14.49 |
| | October-09 | 16.36 | 31.40 | 7.19 | 84.20 | 136.64 | 0.44 | 1.86 | 7.30 | 72.47 | 7.74 | 0.75 | 9.70 | 8.26 | 7.02 |
| | November-09 | 15.83 | 34.40 | 8.70 | 64.30 | 137.40 | 0.24 | 1.26 | 2.33 | 65.85 | 5.94 | 0.60 | 14.45 | 9.33 | 21.70 |
| | March-10 | 19.72 | 34.60 | 4.69 | 168.25 | 171.93 | 3.33 | 9.01 | 18.33 | 145.09 | 4.50 | 1.75 | 40.14 | 10.91 | 11.64 |
| | March-10 | 19.72 | 34.60 | 4.69 | 168.25 | 132.46 | 4.51 | 12.90 | 8.11 | 122.01 | 4.90 | 0.21 | 12.67 | 8.57 | 34.57 |
| | May-10 | 13.62 | 21.97 | 5.17 | 52.25 | 120.39 | 2.10 | 12.18 | 4.35 | 131.85 | 2.09 | 2.12 | 15.18 | 3.91 | 6.00 |
| | July-10 | 8.84 | 36.10 | 6.47 | 167.50 | 12.91 | 0.63 | 4.04 | 2.80 | 63.50 | 6.68 | 0.36 | 22.11 | 3.94 | 11.59 |
| | August-10 | 8.84 | 36.10 | 6.47 | 167.50 | 116.23 | 0.35 | 0.38 | 41.48 | 68.48 | 4.44 | 1.81 | 24.63 | 4.17 | 5.00 |
| | October-10 | 16.58 | 37.05 | 4.45 | 69.05 | 171.75 | 1.12 | 5.02 | 27.31 | 127.03 | 1.70 | 1.38 | 3.86 | 3.29 | 13.42 |
| | November-10 | 17.77 | 36.20 | 5.59 | 198.50 | 17.08 | 2.00 | 3.87 | 2.43 | 52.71 | - | 0.70 | 29.35 | 4.43 | 25.42 |

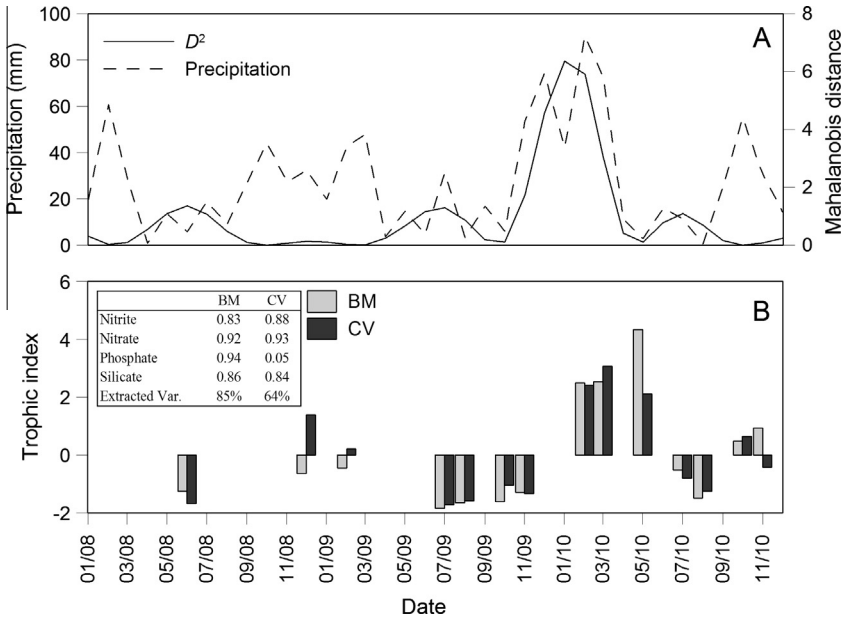


**Fig. 2.** Rainfall regime and nutrient concentration during the sampling period. (A) Mean monthly precipitation level (dashed line) in the Bahía Blanca Estuary and the generalized Mahalanobis distance ($D^2$, solid line) indicating significant anomalies in the time series. (B) Trophic index in the sampling sites during the period investigated. The scores of every nutrient in PC1 and the variance extracted by each PC are shown in the table. Note the conspicuous increase in throphic index immediately after the precipitation peak.

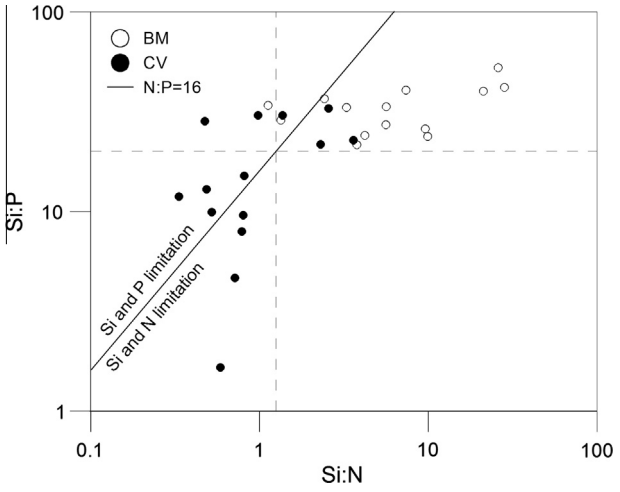


**Fig. 3.** Si:P vs. Si:N diagram showing the logarithmic ratio of nutrients in both sites: BM (white dots) and CV (black dots). Dashed lines correspond to the ideal ratio of nutrients according to Redfield et al. (1963). Lower than Redfield values correspond to Si deficiency with respect to N and P. In addition, the ideal N:P ratio is also represented with a solid line; values at the right side of the line indicate N and Si limitation, while values at the left side of the line indicate P and Si limitation.

in both sites (Mann–Whitney *U*-test, $p < 0.05$) and represented 72% and 82% of total phytoplankton abundance in BM and CV, respectively. Species richness was significantly higher in BM ($t = 2.64$, $df = 26$, $p = 0.014$), and the C:Chl*a* ratio was significantly higher in CV ($t = 2.18$, $df = 26$, $p = 0.04$). Microzooplankton was represented by tintinnids, naked ciliates, heterotrophic dinoflagellates, rotifers and metazoans larvae. Total ciliates (tintinnids and naked ciliates) were the most abundant over the period investigated, and accounted for more than 80% of total abundance. Microzooplankton abundance was significantly higher in BM (mean = 6956 cell $l^{-1}$) than in CV (mean = 4817 cell $l^{-1}$, Mann–Whitney *U*-test, $p < 0.05$). Also, the relationship between mean microzooplankton abundance and biomass during the whole period, was significantly higher in CV (Mann–Whitney *U*-test, $p < 0.05$).

The phytoplankton composition appeared significantly different between sites (ANOSIM test, global $R = 0.15$, $p < 0.001$, Fig. 3). The computed dissimilarity percentage between sites was 75.9%, and the main species contributing to the dissimilarity between groups were *Thalassiosira minima*, nanoflagellates >5 μm and nanoflagellates <5 μm. In BM, phytoplankton was characterized by the diatoms *Thalassiosira minima* and *Paralia sulcata*, while in CV, the dominant groups were nanoflagellates >5 μm and nanoflagellates <5 μm (SIMPER test). Likewise, the microzooplankton composition was significantly different between sites (ANOSIM test, global $R = 0.127$, $p < 0{,}001$). Dissimilarity percentage between sites was 69.5%, while the main species contributing to the dissimilarity were *Tintinnidium balechi*, *Tintinnopsis parva* and *Lohmanniella oviformis*. The dominant species in BM was *T. balechi*, while in CV, *T. balechi* and *L. oviformis* were the most abundant (SIMPER test). The MDS analysis showed the segregation of sampling sites in both phytoplankton and microzooplankton samples (Fig. 4a and b).

### 3.3. Relationship between plankton and the environmental conditions

The response of plankton to environmental conditions was different between sites. The general trend of plankton biomass was estimated as the first PC of three plankton categories (including nanophytoplankton, microphytoplankton and microzooplankton), and extracted 55.9% and 52.6% of total variability of data in BM and CV, respectively. In BM there was no clear relationship between plankton biomass, as indexed by PC1, and the concentration of inorganic nutrients (general trend of nitrate, nitrite, phosphate and silicate) (Fig. 5a). In contrast, in CV the relationship between plankton biomass and the trophic index was quadratic ($R^2 = 0.58$, $df = 10$, *p*-value of quadratic model = 0.013, *p*-value of increase of in $R^2 = 0.003$; Fig. 5b). The size-fraction ratio of phytoplankton showed different responses to nutrients concentration in the sampling sites. In BM, an increase in the concentration of all nutrients (except for ammonium) leaded to a linear increase in the ratio ($R^2 = 0.65$, $df = 12$, $p = 0.000$; Fig. 5c). In contrast, in CV


**Fig. 4.** Multi-dimensional scaling analysis of phytoplankton (A) and microzooplankton (B) with site (BM and CV) as discriminating factor. The analysis is based on the Bray Curtis similarity index. Stress values of the analysis are shown in the right upper corner of each panel.

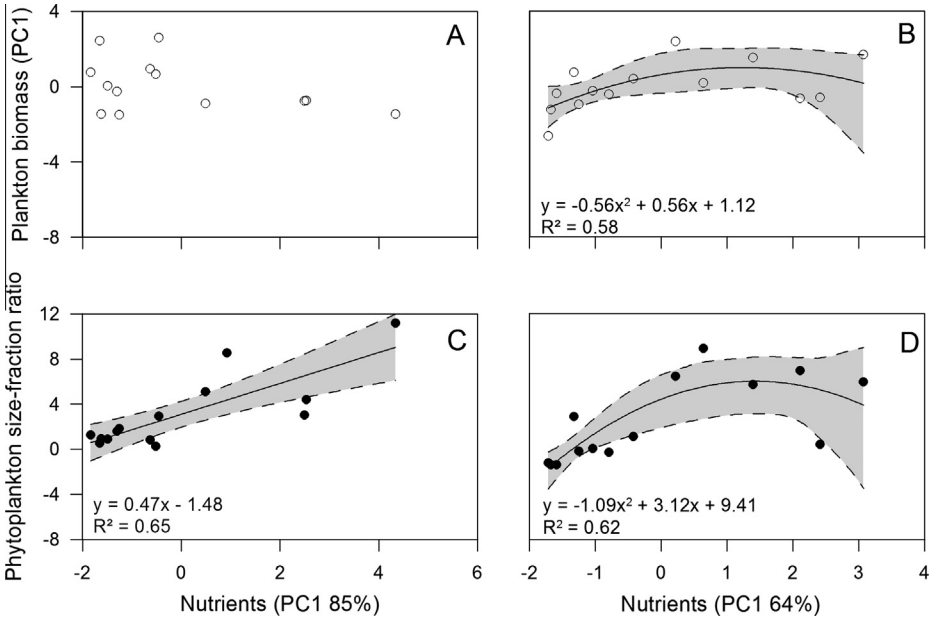


**Fig. 5.** Link between the general trend of plankton biomass (A and B) and the phytoplankton size fraction ratio (C and D) in relation to nutrients in BM (A and C) and CV (B and D). Dashed lines represent confidence interval at 95%. The percentage of variance extracted by PC1 is shown in the *x* axes.

the increase of nutrient concentration beyond a threshold value leaded to a decrease in the phytoplankton size-fraction ratio ($R^2$ = 0.62, *df* = 12, *p*-value of quadratic model = 0.005, *p*-value of increase of in $R^2$ = 0.024; Fig. 5d).

The highest phytoplankton growth rate in CV was concomitant with high values of phosphorous, silicate and ammonium and low values of salinity and microzooplankton biomass, while in BM, the highest values were observed in concurrence with high values of nitrate, nitrite, phosphorous and silicate (Table 1). Although the phytoplankton growth rate was similar in both sites, it showed different relationship with nutrients. In BM, a linear relationship was noticed between the phytoplankton growth rate and the first principal component of nutrient concentration, which summarized the main variance of all nutrients included in the analysis (Fig. 6a and b). In turn, in CV the phytoplankton growth rate was linearly correlated with the second principal component which explained mainly the variance of phosphate (Fig. 6c and d). The rate of microzooplankton grazing did not differ significantly between sites. The averaged proportion of primary production consumed by microzooplankton (m/μ) was 87.6% in BM and 72.3% in CV. The contribution of each nutrient to the formation of PC1 and PC2 are given in Table 2. The relationship between phytoplankton growth rate and temperature is shown in Fig. 7. We noticed that most values were below the maximal growth rate according to Eppley (1972) and Bissinger et al. (2008), however in CV, at times, the rate surpassed the predicted maximal growth rate.

Multivariate drivers of microplankton were depicted by the path analysis (Fig. 8a and b). In BM, path analysis showed that microzooplankton is modulated by the combination of temperature, salinity and dissolved oxygen, and showed trophic interaction with microphytoplankton. The variability of microphytoplankton appeared linked with phosphate concentration and the ecological interactions with both microzooplankton and nanophytoplankton. In turn, the nanophytoplankton variability was linked with the variability of temperature and phosphate. In clear contrast, the configuration of the highly eutrophic site, CV, showed enhanced effects of dissolved oxygen and temperature on microplankton communities. The most conspicuous change was noticed in the temperature effect on the three groups, nanophytoplankton, microphytoplankton and microzooplankton. Under this eutrophic conditions, it was noticeable the enhanced influence of silicates on microphytoplankton, while nanophytoplankton was further affected by nitrates + nitrites, dissolved oxygen and microzooplankton.

## 4. Discussion

### 4.1. Sewage-driven changes in plankton community

In the Bahía Blanca Estuary, nutrient loading from sewage effluents supported a higher number of phytoplankton cells, and resulted in profound changes in plankton composition favoring

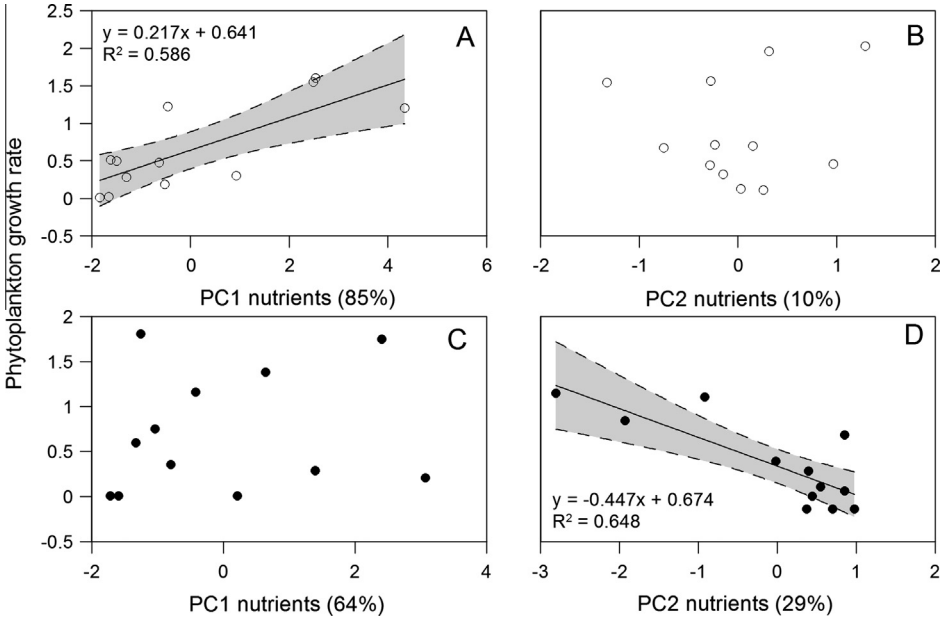


**Fig. 6.** Link between the phytoplankton growth rate and the concentration of nutrients in BM (A and B) and CV (C and D). The general trend of nutrients is represented by the first two components (PC1 and PC2) of the nutrient matrix (including nitrite, nitrate, phosphate and silicate). Dashed lines represent confidence interval at 95%. The percentage of variance extracted by PC1 is shown in the *x* axes.

**Table 2**
Contribution of dissolved inorganic nutrients (PCA scores) to the formation of PC1 and PC2 in BM and CV.

| | BM | | CV | |
|---|---|---|---|---|
| | PC1 | PC2 | PC1 | PC2 |
| Nitrite | 0.83 | 0.45 | 0.88 | 0.19 |
| Nitrate | 0.92 | −0.08 | 0.93 | 0.18 |
| Phosphate | 0.94 | 0.02 | 0.05 | −0.95 |
| Silicate | 0.86 | −0.38 | 0.84 | −0.34 |

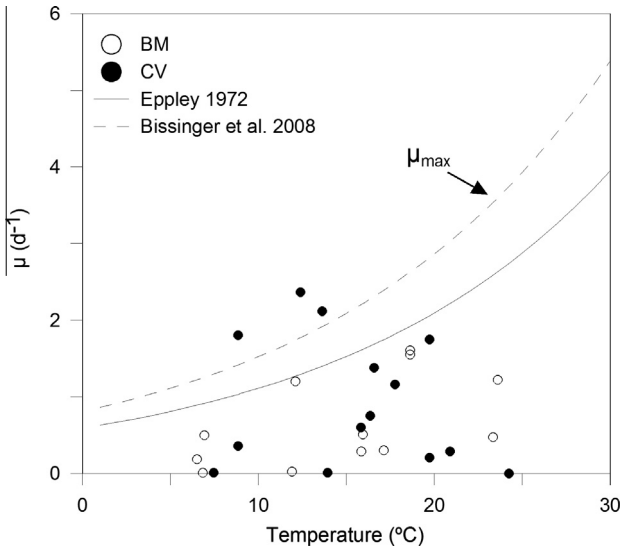


**Fig. 7.** Phytoplankton growth rate ($\mu$) as a function of seawater temperature in both sampling sites BM (white dots) and CV (black dots) and the predicted response of the phytoplankton growth rate to temperature for phototrophic organisms by Eppley, 1972 (solid line) and Bissinger et al., 2008 (dashed line). Note that in CV, the phytoplankton growing rate can potentially surpass the predicted maximum $\mu$ ($\mu_{max}$). This points that at times, the joint effect of higher resource availability and smaller phytoplankton body size in CV can distort the predicted response of growth rate to temperature.

small-sized organisms. We observed that the C:Chl*a* ratio of nanophytoplankton was significantly higher in the sewage-affected area. The environmental conditions found, e.g., extreme ammonium concentration, may lead to the inhibition of the photosynthetic system of phytoplankton (Azov and Goldman, 1982). In fact, empirical evidence shows that ammonium concentration exceeding 100 μM, triggers a rapid reduction of chlorophyll *a* content of phytoplankton (Abeliovich and Azov, 1976). Also, field and laboratory work showed that increasing ammonium concentration lead to a reduction on chlorophyll *a*, abundance and diversity of estuarine phytoplankton (Livingston et al., 2002). The authors recommend that ammonium concentration should not exceed 110 μM, in order to retrieve pre-eutrophication conditions. During our study we found high ammonium concentration that reached 170 μM, which along with high pH variability in CV may yield a higher C:Chl*a* ratio and lower species richness. In addition, the phytoplankton concentration was significantly higher in the highly eutrophic area, providing a greater concentration of potential prey, however the abundance of microzooplankton was significantly lower; such pattern is in agreement with previous observations in the area (Barría de Cao et al., 2003). Similar effects have been shown on mesozooplankton, which exhibited alterations in species composition and abundance in response to sewage effects (Biancalana et al., 2012; Dutto et al., 2012). We hypothesize that the high concentration of ammonium may explain the low microzooplankton abundance in this site, given the known toxic effect on ciliates (Xu et al., 2004; Klimek et al., 2012). The lower consumer density and similar grazing pressure with respect to the control site, along with the occurrence of exceptionally high phytoplankton growth rate draws attention to uncoupling producer – consumer interactions promoted by anthropogenic pollution.

During the survey, oxygen concentration in the surface layer of the highly eutrophic site was significantly lower, and sporadically evidenced hypoxic conditions. Heavy eutrophication is acknowledged to trigger hypoxia conditions in bottom waters (Diaz and Rosenberg, 2008), which warns on the likely threatening status of benthic communities in CV. Coastal hypoxia due to eutrophication might be exacerbated by reduced oxygen solubility due to

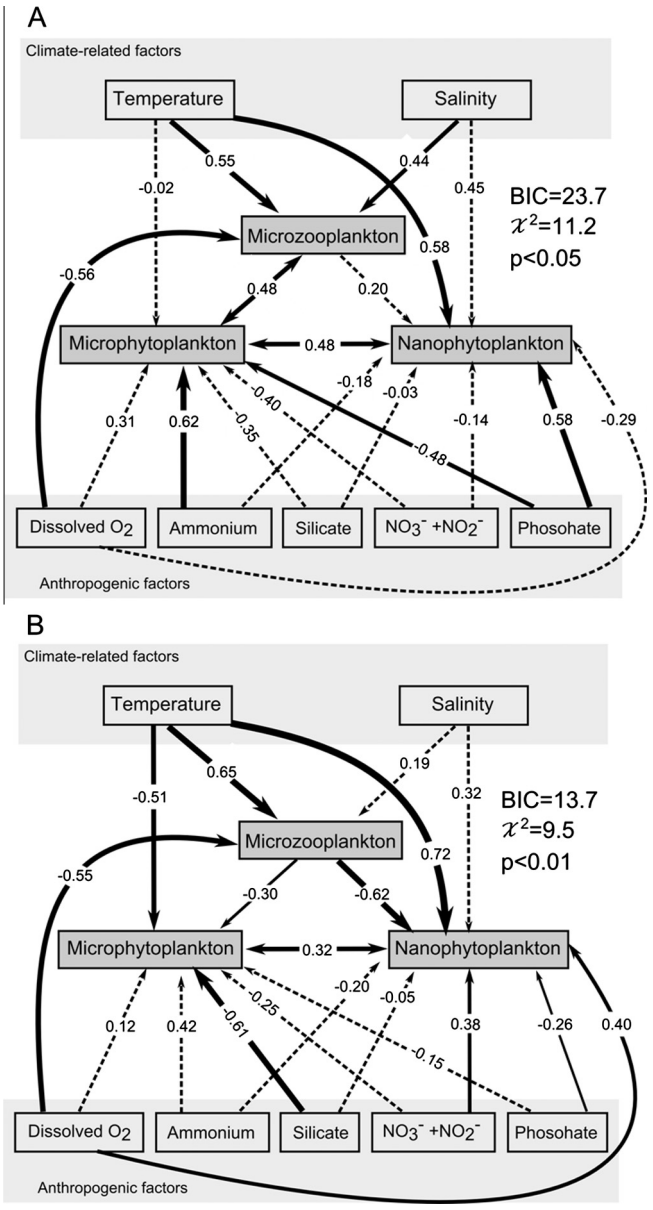


**Fig. 8.** Path diagrams showing the effects of climate-related, i.e. temperature and salinity, and anthropogenic, i.e. dissolved oxygen concentration and nutrient loading, factors on microplankton communities. Solid paths are statistically significant ($p < 0.05$), whereas dashed lines are not. At each significant path the standardized coefficients are displayed. The models correspond to two scenarios of contrasting exposure to (A) low and (B) high anthropogenic eutrophication.

ocean warming (Shaffer et al., 2009), further reducing the habitat range of benthic and pelagic species.

### 4.2. Nutrient stoichiometry and phytoplankton metabolism

Eutrophication of coastal areas stimulates phytoplankton growth and may disrupt the balance between plankton production and metabolism (Cloern, 2001). Given that the metabolic rate is constrained by environmental stoichiometry of nutrients (Brown et al., 2004), the pool of the limiting nutrient dictates the rate at which inorganic nutrients are transformed into phytoplankton biomass. Although the nutrient pool in the highly eutrophic site, CV, was consistently higher than in BM, element stoichiometry showed substantial deviations from the Redfield ratio (Redfield et al., 1963). This is consistent with previous findings showing that human activities on coastal areas have intensified the supply rate of nitrogen and phosphorous in many estuaries worldwide (Fohrer and Chícharo, 2012). According to our results, phosphorous appears as a primary trigger for phytoplankton growth in both areas, although in the highly eutrophic site, the role of silicate appears also relevant. The altered nutrient stoichiometry in this area, i.e. excess nitrogen and phosphorous with respect to silica, shifted the community from the typical dominance of diatoms (Guinder et al., 2010) towards the dominance of unidentified nanoflagellates. Further agents can magnify the input of phosphorous from wastewater, as the lack of vegetation in the urbanized shores (Reddy et al., 1999) and the increase of precipitation level (Sánchez-Carrillo et al., 2009). Changes on nutrient supply ratios and the subsequence habitat deterioration have motivated the implementation of restoration policies in a number of estuaries (Borja et al., 2010). However, the effectiveness of habitat recovering depends on the proper transfer of ecological knowledge to policy managers (Palmer, 2009). In this line, our study provides supporting information for the application of management policies that might reduce habitat lost in the future. The microplankton dynamics in the study area is exposed to the occurrence of phosphorous pulses; the effect of which might favor exceptionally high growth rates and stimulate the development of opportunistic blooming species (e.g. nanoflagellates and mixotrophic-generalist ciliates such as *Lohmaniella oviformis*). As shown by our results, nutrient pulses are shaped by rainfall regime and sewage effluents, and their synergies are critical to fully understand, and eventually predict, plankton productivity in the estuary.

Body size is acknowledged to constrain metabolic rate, and according to the metabolic theory of ecology (Brown et al., 2004), smaller organisms tend to show higher maximum growth rates than larger organisms. In CV, the phytoplankton growth rate can potentially surpass the predicted response of the growth rate to temperature for phototrophic organisms (Eppley, 1972). The predictive equation depicted by Eppley was recently revised by Bissinger et al. (2008). The authors applied quantile regression using an exhaustive data set and came into a more precise predictive equation, which defines higher $\mu_{max}$ values than the ones described by Eppley. Yet, the phytoplankton growth rate we observed in the highly eutrophic site, surpass the predictive curve stated by Bissinger et al. (2008). This suggests that at times, the joint effect of higher eutrophication level and smaller phytoplankton body size can distort the predicted response of growth rate to temperature. While nutrient loading can shift the size scaling of metabolic rate of autotrophic plankton (Irwin et al., 2006), the specific physiological response to changes in resource supply and the consequent outcome on population abundance remain a major endeavor in aquatic ecology (Cermeño et al., 2008). It is worth noting however, that the phytoplankton growth rate in Eppley (1972) and Bissinger et al. (2008) was based on abundance, while the rates obtained in this study were based on chlorophyll *a*. Although this may question the validity of the comparison, chlorophyll *a* has been identified as a reliable proxy for autotrophic plankton density in the Bahía Blanca Estuary (Popovich and Marcovecchio, 2008), and thus one could assume that the outgoing results from both estimations will be roughly the same (Landry and Hassett, 1982).

Implications of changes in nutrients balance are critical for food web functioning as they may shift the temperature dependence of metabolic rate. Indeed, recent studies pointed out that nutrients supply, but not temperature, is the main factor controlling phytoplankton growth rate in marine environments (Marañón et al., 2012, 2014). In agreement with this, our results showed that although nutrients concentration in CV was high, phytoplankton growth was constrained by the concentration of phosphorous and silicate, while temperature appeared to have no effect on the metabolic rate. The structuring role of nutrients supply would be

further intensified by low grazing pressure (Irwin et al., 2006). Although microzooplankton grazing rate was similar in both sites, the proportion of primary production consumed by microzooplankton (m/μ) and the concentration of micro-sized grazers was lower in CV. The modification of the predicted response of phytoplankton growth to temperature under disturbed nutrient stoichiometry and low grazing pressure highlights the need to include input variables and scaling coefficients for realistically model the response of plankton metabolism to temperature in highly eutrophic environments.

In estuaries and other coastal areas, heavy rainfall and freshwater flowing events create pulses of dissolved nutrients in the water column, boosting primary and secondary productivity (Kimmerer, 2002; Hoover et al., 2006). Resource pulses challenge local adaptation of species and have the potential to permeate the entire community by affecting bottom up regulation and propagating the effect throughout the food web (Holt, 2008). Although the Bahía Blanca Estuary is a highly eutrophic system, nutrient pulses coupled to extreme precipitation events magnify bottom-up controls on phytoplankton. For instance, in the BM site, even the highest nutrient concentration registered after the heavy rainfall season in spring 2009-summer 2010, resulted in a proportional positive response of plankton biomass. Conversely, in the highly eutrophic site, CV, the response of plankton to growing eutrophication evidenced that beyond certain threshold value (nitrite: 3 μM, nitrate: 9 μM, phosphate: 18 μM, and silicate: 140 μM), nutrient concentration seems to impair plankton development. Moreover, the size fraction ratio of phytoplankton showed a similar response, suggesting that excessive nutrients load, i.e. sewage pollution, inhibits its growth, although smaller autotrophic cells might benefit from nutrient enrichment. The functional responses of plankton observed in both scenarios points that in the highly eutrophic area, plankton communities are close to carrying capacity and thus has lower reactivity potential to face environmental perturbations.

### 4.3. Ecological implications of sewage pollution

As shown by the path analysis, microplankton displayed a close coupling with climate and anthropogenic influence in the highly eutrophic area. In addition to the direct influence of climate on microzooplankton, the path model in CV showed that nanophytoplankton mediate the influence of climate on microherbivores. In the same way, phytoplankton biomass was directly and indirectly (via microherbivores) affected by climate. This contrast with the pattern identified in BM where phosphate was the main factor controlling phytoplankton biomass, while climate appears as the main factor controlling microzooplankton. Only the micro-sized fraction of phytoplankton was directly associated with ammonium and indirectly associated with climate via microherbivores. These results point that the entire microplankton community is tightly regulated by climate conditions, via temperature, and by anthropogenic stress, portrayed by nutrients concentration. The close coupling between plankton dynamics and environmental drivers in the sewage-affected area within the Bahía Blanca Estuary warns the potential to enhanced instability of pelagic communities in response to the increased uncertainty under future scenarios of climate changes.

## 5. Concluding remarks

Our results provide quantitative evidence on structural and functional responses of microplankton communities to perturbations of nutrient balance. That is, plankton structure was modified by the partial replacement of diatoms by small-sized, non siliceous algae, while mixotrophic protists took advantage over the typical estuarine microzooplankton assemblages. Functional responses to severe eutrophication were evidenced by changes in the temperature dependence of the metabolic rate and lower reactivity potential to rainfall-driven nutrient pulses and stronger climate regulation. The wide ecological implications of coastal eutrophication along with long-term regional climate change (Guinder et al., 2010) may trigger non-linear feedbacks on higher trophic levels, and ultimately hamper the implementation of prediction and management tools.

## Acknowledgments

We thank Camilo Bernardez, Enio Redondo and Alberto Conte for the technical support and assistance during field sampling. We are grateful to Paula Pratolongo, Hugo Freije and Carla Spetter for comments on the early version of this manuscript. We thank the Center for Renewable Natural Resources of the Semiarid Zone, CONICET (CERZOS) and the National Oceanic and Atmospheric Administration (NOAA), for providing climatic data. The study was supported by the Agencia Nacional de Promoción Científica y Tecnológica (FONCYT-PICT 1713), by the Instituto Argentino de Oceanografía, (IADO-CONICET) and by scholarships from CONICET, Argentina. The research of JCM is a contribution to the EU project OCEAN-CERTAIN (European Commission, OCEAN-CERTAIN, FP7-ENV-2013-6.1-1; no: 603773).

## References

Abeliovich, A., Azov, Y., 1976. Toxicity of ammonia to algae in sewage oxidation ponds. Appl. Environ. Microbiol. 31, 801–806.
Alsterberg, C., Eklöf, J.S., Havenhand, J., Sundbäck, K., Gamfeldt, L., 2013. Consumers mediate the effects of experimental ocean acidification and warming on primary producers. Proceedings of the National Academy of Sciences U.S.A. vol. 110(21), pp. 8603–8608.
APHA-AWWA-WEF, 1998. Standard Methods for the Examination of Water and Wastewater, 20th ed. Method 4500Cl B. American Public Health Association and American Water Works Association and Water Environment Federation, Washington, DC, USA.
Azov, Y., Goldman, J.C., 1982. Free ammonia inhibition of algal photosynthesis in intensive cultures. Appl. Environ. Microbiol. 43, 735–739.
Baldini, M.D., Cubitto, M.A., Chiarello, M.N., Cabezali, C.B., 1999. Water quality for aquaculture development in Bahía Blanca estuary, Argentina. Bacteriological studies. Rev. Argentina Microbiol. 31, 19–24.
Barría de Cao, M.S., Pettigrosso, R.E., Parodi, E., Freije, R.H., 2003. Abundance and species composition of planktonic Ciliophora from the wastewater discharge zone in the Bahía Blanca Estuary, Argentina. Iheringia, Série Zoolgia, Porto Alegre 93 (3), 229–236.
Biancalana, F., Menéndez, M.C., Berasategui, A.A., Fernández Severini, M.D., Hoffmeyer, M.S., 2012. Sewage pollution effects on mesozooplankton structure in a shallow temperate estuary. Environ. Monit. Assess. 184, 3901–3913.
Bissinger, J.E., Montagnes, D.J.S., Sharples, J., Atkinson, D., 2008. Predicting marine phytoplankton maximum growth rates from temperature: improving on the Eppley curve using quantile regression. Limnol. Oceanogr. 53, 487–493.
Borel, C.M., Gómez, E.A., 2006. Palinología del Holoceno del Canal del Medio, estuario de Bahía Blanca, Buenos Aires, Argentina. Ameghiniana 43, 399–412.
Borja, A., Dauer, D.M., Elliott, M., Simenstad, C.A., 2010. Medium- and long-term recovery of estuarine and coastal ecosystems: patterns, rates and restoration effectiveness. Estuaries Coasts 33, 1249–1260.
Brown, J.H., Gillooly, J.F., Allen, A.P., Savage, V.M., West, G.B., 2004. Toward a metabolic theory of ecology. Ecology 85, 1771–1789.
Cermeño, P., Marañón, E., Harbour, D.S., Figueiras, F.G., Crespo, B.G., Huete, M., Varela, M., Harris, R.P., 2008. Resource levels, allometric scaling of phytoplankton abundance and marine phytoplankton diversity. Limnol. Oceanogr. 53 (1), 312–318.
Clarke, K.R., Gorley, R.N., 2006. PRIMER version 6: User Manual/Tutorial. PRIMER-E Ltd., Plymouth.
Clarke, K.R., Warwick, R.M., 1994. Change in Marine Communities: An Approach to Statistical Analysis and Interpretation, first ed. Plymouth Marine Laboratory, Plymouth, UK.
Cloern, J.E., 2001. Our evolving conceptual model of the coastal eutrophication problem. Mar. Ecol. Prog. Ser. 210, 223–253.
Diaz, R.J., Rosenberg, R., 2008. Spreading dead zones and consequences for marine ecosystems. Science 321, 926–928.
Dutto, M.S., López Abbate, M.C., Biancalana, F., Berasategui, A.A., Hoffmeyer, M.S., 2012. The impact of sewage on environmental quality and the

mesozooplankton community in a highly eutrophic estuary in Argentina. ICES J. Mar. Sci. 69 (3), 399–409.
Elser, J.J., Peace, A.L., Kyle, M., Wojewodzic, M., McCrackin, M.L., Andersen, T., Hessen, D.O., 2010. Atmospheric nitrogen deposition is associated with elevated phosphorus limitation of lake zooplankton. Ecol. Lett. 13, 1256–1261.
Eppley, R.W., 1972. Temperature and phytoplankton growth in the sea. Fish. Bull. 70, 1063–1085.
Fohrer, N., Chícharo, L., 2012. Interaction of river basins and coastal waters – an integrated ecohydrological view. In: McLusky, D., Wolanski, E. (Eds.), Treatise on Estuarine and Coastal Science, Volume 10: Ecohydrology and Restoration. Elsevier, Oxford, chapter 10.06.
Freije, R.H., Spetter, C.V., Marcovecchio, J.E., Popovich, C.A., Botté, S.E., Negrín, V., Arias, A., Delucchi, F., Asteasuain, R.O., 2008. Water chemistry and nutrients in the Bahía Blanca Estuary. In: Neves, R., Baretta, J., Mateus, M. (Eds.), Perspectives on Integrated Coastal Zone Management in South America. IST Press, Scientific Publishers, Lisbon, Portugal, pp. 243–256.
Gonzalez, A., Loreau, M., 2009. The causes and consequences of compensatory dynamics in ecological communities. Annu. Rev. Ecol. Evol. Syst. 40, 393–414.
Guinder, V.A., Popovich, C.A., Molinero, J.C., Perillo, G.M.E., 2010. Long-term changes in phytoplankton phenology and community structure in the Bahía Blanca Estuary, Argentina. Mar. Biol. 157 (12), 2703–2716.
Guinder, V.A., Popovich, C.A., Molinero, J.C., Marcovecchio, J., 2013. Phytoplankton summer bloom dynamics in the Bahía Blanca Estuary in relation to changing environmental conditions. Cont. Shelf Res. 52, 150–158.
Hasle, G., 1978. Concentrating phytoplankton. Settling. The inverted microscope method. In: Sournia, A. (Ed.), Phytoplankton Manual. Monographs on Oceanographic Methodology, vol. 6. UNESCO, Paris, pp. 88–96.
Hillebrand, H., Dürselen, C.-D., Kirschtel, D., Pollingher, U., Zohary, T., 1999. Biovolume calculation for pelagic and benthic microalgae. J. Phycol. 35, 403–424.
Hoffmeyer, M.S., 2004. Decadal change in zooplankton seasonal succession in the Bahía Blanca Estuary, Argentina, following introduction of two zooplankton species. J. Plankton Res. 26, 181–189.
Hoffmeyer, M.S., Barría de Cao, M.S., 2007. Zooplankton assemblages from a tidal channel in the Bahía Blanca Estuary, Argentina. Braz. J. Oceanography 55 (2), 97–107.
Holt, R.D., 2008. Theoretical perspectives on resource pulses. Ecology 89 (3), 671–681.
Hoover, R.S., Hoover, D., Miller, M., Landry, M.R., DeCarlo, H., Mackenzie, S.T., 2006. Zooplankton response to storm runoff in a tropical estuary: bottom-up and top-down controls. Mar. Ecol. Prog. Ser. 318, 187–201.
Ibanez, F., 1981. Immediate detection of heterogeneities in continuous multivariate oceanographic recordings. Application to time series analysis of changes in the bay of Villefranche sur mer. Limnol. Oceanogr. 26, 336–349.
Irwin, A.J., Finkel, Z.V., Schofield, O.M.E., Falkowski, P.G., 2006. Scaling-up from nutrient physiology to the size-structure of phytoplankton communities. J. Plankton Res. 28, 459–471.
Kimmerer, W.J., 2002. Effects of freshwater flow on abundance of estuarine organisms: physical effects or trophic linkages? Mar. Ecol. Prog. Ser. 243, 39–55.
Klimek, B., Fyda, J., Pajdak-Stós, A., Kocerba, W., Fiałkowska, E., Sobczyk, M., 2012. Toxicity of ammonia nitrogen to ciliated protozoa *Stentor coeruleus* and *Coleps hirtus* isolated from activated sludge of wastewater treatment plants. Bull. Environ. Contam. Toxicol. 89, 975–977.
Landry, M.R., Hassett, R.P., 1982. Estimating the grazing impact of marine microzooplankton. Mar. Biol. 67, 283–288.
Lara, R.J., Gomez, E.A., Pucci, A.E., 1985. Organic matter, sediment particle size and nutrient distributions in a sewage affected shallow channel. Mar. Pollut. Bull. 16 (9), 360–364.
Livingston, R.J., Prasad, A.K., Niu, X., McGlynn, S.E., 2002. Effects of ammonia in pulp mill effluents on estuarine phytoplankton assemblages: field descriptive and experimental results. Aquat. Bot. 74, 343–367.
Lorenzen, C.J., Jeffrey, S.W., 1980. Determination of chlorophyll in seawater. UNESCO Tech. Paper Mar. Sci. 35, 1–20.
Marañón, E., Cermeño, P., Latasa, M., Tadonléké, R.D., 2012. Temperature, resources, and phytoplankton size structure in the ocean. Limnol. Oceanogr. 57 (5), 1266–1278.
Marañón, E., Cermeño, P., Huete-Ortega, M., López-Sandoval, D.C., Mouriño-Carballido, B., Rodríguez-Ramos, T., 2014. Resource supply overrides temperature as a controlling factor of marine phytoplankton growth. PLoS ONE 9 (6), e99312. http://dx.doi.org/10.1371/journal.pone.0099312.
Marcovecchio, J.E., Botté, S.E., Delucchi, F., Arias, A., Fernández Severini, M., De Marco, S., Tombesi, N., Andrade, S., Ferrer, L., Freije, R.H., 2008. Pollution processes in Bahía Blanca estuarine environment. In: Neves, R., Baretta, J.W., Mateus, M. (Eds.), Perspectives on Integrated Coastal Zone Management in South America. IST Press, Scientific Publishers, Lisbon, Portugal, pp. 301–314.
Menden-Deuer, S., Lessard, E.J., 2000. Carbon to volume relationships for dinoflagellates, diatoms, and of the protist plankton. Limnol. Oceanogr. 45, 569–579.
Montecinos, A., Díaz, A., Aceituno, P., 2000. Seasonal diagnostic and predictability of rainfall in subtropical South America based on tropical pacific SST. J. Clim. 13, 746–758.
Paerl, H.W., Valdes, L.M., Peierls, B.L., Adolf, J.E., Harding Jr., L.W., 2006. Anthropogenic and climatic influences on the eutrophication of large estuarine ecosystems. Limnol. Oceanogr. 51 (1), 448–462.
Palmer, M.A., 2009. Reforming watershed restoration: science in need of application and applications in need of science. Estuaries Coasts 32, 1–17.
Peres-Neto, P., Legendre, P., Dray, S., Borcard, D., 2006. Variation partitioning of species data matrices: estimation and comparison of fractions. Ecology 87, 2614–2625.
Perillo, G.M.E., Piccolo, M.C.E., Parodi, E., Freije, R.H., 2001. The Bahía Blanca Estuary, Argentina. In: Seeliger, U., Kjerfve, B. (Eds.), Coastal Marine Ecosystems of Latin America. Springer-Verlag, Berlin, pp. 205–217.
Popovich, C.A., Marcovecchio, J.E., 2008. Spatial and temporal variability of phytoplankton and environmental factors in a temperate estuary of South America (Atlantic coast, Argentina). Cont. Shelf Res. 28, 236–244.
Prairie, J.C., Sutherland, K.R., Nickols, K.J., Kaltenberg, A.M., 2012. Biophysical interactions in the plankton: a cross-scale review. Limnol. Oceanography: Fluids Environ. 2, 121–145.
Rabalais, N.N., 2004. Eutrophication. In: Robinson, A.R., McCarthy, J., Rothschild, B.J. (Eds.), The Global Coastal Ocean: Multiscale Interdisciplinary Processes. The Sea. Harvard University Press, Cambridge, MA, pp. 819–865.
Rabalais, N.N., Turner, R.E., Díaz, R.J., Justić, D., 2009. Global change and eutrophication of coastal waters. ICES J. Mar. Sci. 66, 1528–1537.
Reddy, K.R., Kadlec, R.H., Flaig, E., Gale, P.M., 1999. Phosphorus retention in streams and wetlands: a review. Environ. Sci. Technol. 29, 83–146.
Redfield, A.C., Ketchum, B.H., Richards, F.A., 1963. The influence of organisms on the composition of sea-water. In: Hill, M.N. (Ed.), The Sea. John Wiley & Sons, New York, pp. 12–37.
Sánchez-Carrillo, S., Sanchez-Andres, R., Alatorre, L.C., Angeler, D.G., Alvarez-Cobelas, M., Arreola-Lizarraga, J.A., 2009. Nutrient fluxes in a semi-arid microtidal mangrove wetland in the Gulf of California. Estuar. Coast. Shelf Sci. 82, 654–662.
Scheffer, M., Carpenter, S.R., 2003. Catastrophic regime shifts in ecosystems: linking theory to observation. Trends Ecol. Evol. 18 (12), 648–656.
Shaffer, G., Olsen, S.M., Pedersen, J.O.P., 2009. Long-term ocean oxygen depletion in response to carbon emissions from fossil fuels. Nat. Geosci. 2, 105–109.
Spetter, C.V., Popovich, C.A., Arias, A., Asteasuain, R.O., Freije, R.H., Marcovecchio, J.E., 2015. Role of Nutrients in phytoplankton development during a winter diatom bloom in a eutrophic South American Estuary (Bahía Blanca, Argentina). J. Coastal Res. 31, 76–87.
Sterner, R.W., Elser, J.J., 2002. Ecological Stoichiometry: The Biology of Elements from Molecules to the Biosphere. Princeton University Press, Princeton.
Strom, S., 2002. Novel interactions between phytoplankton and microzooplankton: their influence on the coupling between growth and grazing rates in the sea. Hydrobiologia 480, 41–54.
Taylor, A.H., Allen, J.I., Clark, P.A., 2002. Extraction of a weak climatic signal by an ecosystem. Nature 416, 629–632.
Xu, H., Song, W., Warren, A., 2004. An investigation of the tolerance to ammonia of the marine ciliate *Euplotes vannus* (Protozoa, Ciliophora). Hydrobiologia 519, 189–195.